TÍTULO: Diseño del receptor óptico integrado DC-20 GHz basado en la tecnología SiGe BiCMOS.

AUTORES:

1. Artyom S. Koryakovtsev.

2. Andrey A. Kokolov.

3. Alexey V. Pomazanov.

4. Fiodor I. Sheyerman.

5. Leonid I. Babak.

RESUMEN: Se describe el diseño de receptor integrado con ancho de banda de DC-20 GHz basado en la tecnología SiGe BiCMOS de 0.25 µm. Se obtuvieron como resultados: la ganancia hasta 20 GHz es aproximadamente 22-2 5dB, la ganancia de transimpedancia es 61-65 dBΩ dentro del ancho de banda, y el consumo actual es de 60 mA. La potencia de salida a 20 GHz es -4.5 dBm, la amplitud rms de salida es de 0.3 V con una carga de 50 Ohmios, ruido de corriente referido a la entrada in = 15.6 pA / √Hz, el retardo de grupo para el receptor óptico es de 30 ± 2 ps. El dispositivo puede utilizarse en sistemas de telecomunicaciones de banda ancha, líneas de transmisión de señales de microondas dentro de objetos grandes, antenas de matriz en fase y mucho más.

PALABRAS CLAVES: amplificador de transimpedancia, fotónica de microondas, fotodiodo, amplificador diferencial, SiGe BiCMOS.

TITLE: Design of integrated optical Receiver DC-20 GHz based on SiGe BiCMOS technology.

AUTHORS:

1. Artyom S. Koryakovtsev.

2. Andrey A. Kokolov.

3. Alexey V. Pomazanov.

4. Feodor I. Sheyerman.

5. Leonid I. Babak.

ABSTRACT: The integrated receiver design with DC-20 GHz bandwidth based on 0.25 μm SiGe BiCMOS technology is described. The following results were obtained: the gain up to 20 GHz is approximately 22-2 5dB, the transimpedance gain is 61-65 dBΩ within the bandwidth, and the current consumption is 60 mA. The output power at 20 GHz is -4.5 dBm, the rms output amplitude is 0.3 V with a load of 50 Ohms, current noise referred to the input in = 15.6 pA / √Hz, the group delay for the receiver optical is 30 ± 2 ps. The device can be used in broadband telecommunications systems, microwave signal transmission lines within large objects, phased array antennas and much more.

KEY WORDS: transimpedance amplifier, microwave photonics, photodiode, differential amplifier, SiGe BiCMOS.

INTRODUCTION.

Creating multi-service civil and military-oriented complexes of radiolocation, navigation, and communication on the basis of multi-channel active electronically scanned arrays (AESA), including digital ones (DAESA), are figures prominently in the development of state-of-the-art microwave radioelectronic and telecommunication systems.

Today, these microwave range complexes have usually been built taking a traditional approach that implies use of only electronic components (discrete semi-conductor and electronic devices, monolithic microwave integrated circuits (MMICs) of radioelectronic devices: amplifiers, mixers, generators, etc.). However, the approach has a number of principal restrictions; therefore, some system parameters necessary in modern facilities cannot be achieved. Thus, an active development of another approach to creating and applying microwave photonic devices and systems is currently underway.

Microwave photonics [1-4] is an interdisciplinary area that combines radioelectronics and optical electronics. This area is very rapidly developing due to the fact that it, on the one hand, allows to introduce microwave components, that previously were complicated or hard if not impossible to create in the microwave range, and on the other hand, it opens new ways to build information and telecommunication systems and networks owing to the increased speed of transferring data (Seeds, 2002; Capmany & Novak, 2007; Coldren, 2010; Awny et al, 2015).

Major advantages of microwave photonic devices and systems are related to the properties of optical fiber: ultralow losses (less than 0.4 dB/km) and dispersion (for microwave signal), ultrabandwidth (is limited by frequency band of modern photodiodes and electrical and optical modulators, reaching 100 GHz and more), immunity to electromagnetic interferences, full galvanic isolation, mechanical flexibility, small weight and sizes.

Use of microwave photonic technologies will allow to increase the working frequency band, stability of main parameters, interference resistance, and to improve weight and size characteristics of systems with AESA receive-transmit modules (TRM), including: reduction of losses in signal transmission lines; enhancing repeatability of amplitude-phase-frequency response (APFR) from channel to channel in the range of working frequencies and temperatures; improving characteristics of electromagnetic compatibility (EC)/ channel interference immunity; enhancing transmitting

capacitance of digital channels for transferring information of monitoring and control systems; possibility for multiplexing, i.e. reducing the number of AESA distribution systems' transmission lines; improving weight-size characteristics of devices for transmitting, receiving, distributing, pickup of signals, and AESA beamformers, etc.

In Russia, the level of research studies in the area under discussion has not been in step with the worldwide level. There are known works, where only application of ready-to-use, usually foreign-made radio-photonic components is under study while constructing different systems.

USA companies achieved the greatest success in microwave photonic technologies and their basic components. Export of devices for converting and transmitting microwave signals across optical lines is limited of intended purpose that precludes their potential extensive use.

However, series-produced foreign microwave photonic components (laser emitters and photo-receivers, modulators, etc.) have considerable sizes that prevents their use in microwave transceivers with AESA, and in airborne ones, in particular. Therefore, advanced countries have recently intensified research studies on creating microwave photonic integrated circuits using microelectronic technologies, where photonic and electronic components (so called nano-photonics or Silicon Photonics) are integrated on one silicon IC (of an area of mm^2 unities). Besides a sharp decrease in sizes and weight, this approach allows to considerably improve many characteristics of fiber-optic system components, as well as for purposes of creating new generation microwave TRM with DAESA. Use of photonic integrated circuits together with MIC based on gallium nitride (GaN) technology is also interesting for the above application, which allows to additionally extend capabilities of components.

A special attention to microwave photonic technologies is also due to, in particular, an increase in the volume of data transferred within Internet, updating standards of transferring IEEE data to 100 Gb/sec (IEEE 802.3ba) and 400 Gb/sec (IEEE P802.3bs). One of methods for increasing the speed of

transferring data is to increase the bandwidth of a single channel through the use of more efficient technology of electrooptical/optoelectronic conversion or use of more complex methods of modulation (for example, pulse-amplitude modulation, QPSK, etc.) (Rito et al, 2016; López et al, 2015).

An analog optical channel for transferring data serves as a basis of any microwave photonic system. It contains a modulator for converting electrical signal into optical, transmission lines (optical fiber) and optical receiver, which makes a reverse conversion of optical signal into electrical.

Generally, optical receiver includes a photodiode (PD) and a transimpedance amplifier (TIA). Photodiode converts optical signal into output current proportionally to the laser flow intensity. The main purpose of TIA is to transform output current of photodiode into output voltage. Magnitude of output voltage to input current ratio is called a transimpedance gain. This coefficient is expressed as a magnitude of output voltage to input current ratio (V_O/I_{IN}), and has Ω or dB·Ω measurement units (Assefa, 2013; Razavi, 2012).

Integration within integrated circuit of such optoelectronic devices as photodiode, laser, modulator, optical waveguide in combination with electronic and, over the longer term, digital devices allows to increase working frequencies up to 54 Gb/sec using 0.25 µm SiGe BiCMOS technology (Yao, 2009; Jalali, 2006). It is achieved largely due to lack of parasitics in wire interconnections and a shorter way from optoelectronic to microelectronic devices.

The purpose of this work is to develop a single-chip integrated optical receiver with up to 20GHz bandwidth on the basis of monolithic 0.25 µm SiGe BiCMOS technology.

DEVELOPMENT.

Integrated microwave photonics.

There are several reasons that preclude a widespread use of microwave photonic systems in real appliances instead of laboratory facilities. Although some characteristics of microwave photonic

systems are vastly superior to those of traditional microwave systems (broad frequency bandwidth, femtosecond delays, pulse shaping), microwave photonic systems basically have small dynamic range; i.e. the losses, while transforming a signal from optical into electrical one and vice versa, are rather high (approximately ~40 dB). Dynamic range is also limited by relatively high noise of receivers and low output power of transmitters.

Other factors, limiting the use of microwave photonic systems, include their cost, reliability, and power consumption. Most microwave photonic systems consist of discrete components: lasers, modulators and detectors connected with optical fiber. First, it causes an increase in sizes, and interconnections using optical fiber reduce reliability. Second, use of discrete components considerably increases the system cost, since the price of components includes the cost of packaging. Nowadays, these reasons do not enable microwave photonic systems to replace conventional, well-developed pure microwave solutions.

Reduction of cost and consumed power, and enhanced reliability will give a great impetus to developing the systems of microwave photonics. Thus, they will be capable of competing with traditional microwave components, currently used to process signals, and not just with coaxial transmission lines. Leading research centers are in general agreement that it can be solved by means of integrating electronic and photonic components [10]. Using the technology of integrated photonics, a decrease in the system size can be achieved, likewise losses between the elements, cost of packaging, and consumed power, since one cooling element will be utilized for several elements (Soref, 2006). Thus, characteristics of radio-photonic systems may be close to those required for use in real systems.

Although, in the beginning the concept of microwave integrated photonics substantially complied with recent tendencies in the technology of large photonic integrated circuits (PICs), there appeared profound differences therein since their area of application, and available market differ. Requirements

for PICs were formed taking into account their use in such digital systems as high-speed optical communication lines and optical interconnections. This concept mostly implies an increase in transmission velocity, number of components, and development of as many functional capabilities (integration of active and passive elements) within a single platform/technology as possible (Soref, 2006; Jalali & Fathpour, 2006). However, now, there is no a unified technological platform that allows to obtain the best parameters in all aspects, therefore, largely integrated PICs often represent a compromise between various parameters that, in its turn, decreases the total effectiveness of the system.

An important objective of microwave photonics is to optimize the system transmission coefficient and obtain a small noise figure that requires minimization of PIC inserted losses. In most cases, it results in strict requirements for losses in waveguides, input/output fiber to PIC couplers. As regards accessibility of PIC technology, nowadays there are such several communities as ePIXfab and Jeppix [14] in Europe, which enable developers to gain an access to manufacturing technologies of optical integrated circuits by means of combining on one wafer designs of several customers (MPW – multiproject wafer), which would be too expensive for single customer (Dumon et al, 2009; Leijtens, 2011). It has already resulted in the growing number of publications about integrated microwave photonic systems and devices, since these initiatives appear.

Structural diagram of optical electronic receiver.

Fig. 1 presents a generalized structural diagram of receiving EPIC, designed to receive and process optical signals within digital systems of transmitting information (Razavi, 2012; Wang, 2018). Optoelectronic (microwave photonic) receiver consists of a reverse biased photodiode (PD) and the respective input voltage bias circuit, transimpedance amplifier (TIA), limiting amplifier (LA), automatic gain control circuit (AGC), clock and data recovery circuit (CDR). Signal from optoelectronic receiver output comes to high-speed analogue-to-digital converter (ADC).

Fig. 1 – Generalized block diagram of receiving EPIC for digital systems of transferring information.
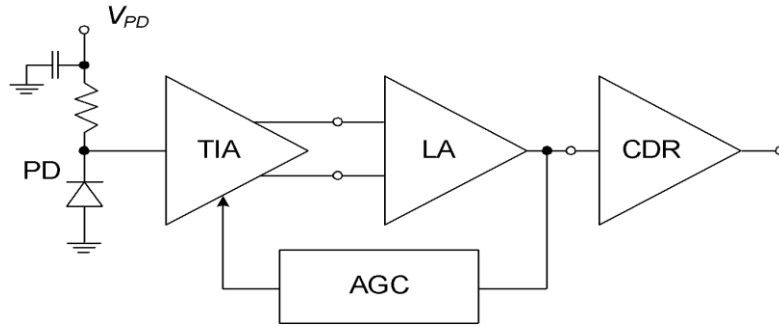

For the system of transmitting analog signal a diagram presented in Fig.1 is reduced to photodiode and TIA, which compensates losses of signal during optoelectronic conversion and amplifies microwave signal to the required level (Wang, 2018).

A generalized block diagram of receiving EPIC for analog signals is given in Fig. 2; usually to achieve the necessary gain TIA involves three stages:

1) Input stage shall have a high gain and minimum added noise, and provide matching with photodiode. Input stage is usually built according to current feedback amplifier circuit, or so called transimpedance amplifier circuit.

2) Post amplifier is required to increase the general TIA gain.

3) Output buffer amplifier shall assure the required level of output power, and, generally, it shall be matched for 50 Ohm load (or 100 Ohm differential load).

Fig. 2 – Generalized block diagram of receiving RIC for analogue systems of transferring information.
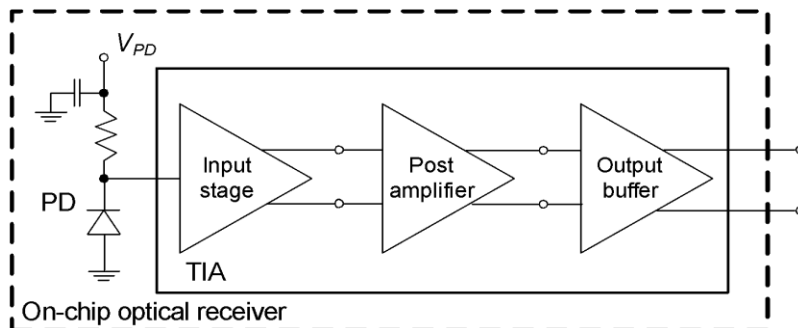
When there are large flows of data at the transmitter and receiver inputs/outputs, the so called Serializer / Deserializer (Ser/Des) integrated circuits are used, which convert the data between serial and parallel interface in both directions.

Transimpedance amplifier: design approaches.

Photodiode converts input optical signal into output current proportionally to the light intensity. The main purpose of TIA is to transform photodiode output current, which occurs therein when optical signal falls to it, into output voltage. A magnitude of output voltage to input current ratio is called a transimpedance gain:

$$Z_T = \left| \frac{V_{out}}{I_{in}} \right|, \qquad (1)$$

where Z_T – transimpedance gain;

V_{out} – TIA output voltage;

I_{in} – TIA input current (or photodiode output current).

Basic characteristics of TIA are as follows [8]:

- Transimpedance gain Z_T, measured in dB·Ω.

- Working frequency band, Δf.

- Noise figure, NF, or integrated noise input current, $I_{n\ in\ ref}$.

- Sensitivity, $P_{in\ min}$.

- Maximum output power, P_{out}.

- Direct current consumption, P_{DC}.

As a rule, noise in TIA is defined by either noise density of input current, or its integral value in the given bandwidth. Input noise current may be presented as a current noise source, added to input of ideal TIA. Virtually all measurements of noise are based upon measuring power of output noise voltage $v_{n,out}$. With the known transimpedance gain Z_T, power of input noise current can be found

(Ahmed, 2013):

$$\left|i_{n,in}\right|^2 = \frac{\left|v_{n,out}\right|^2}{\left|z_T\right|^2}, \qquad (2)$$

where $\left|i_{n,in}\right|^2$ – power of input noise current;

$\left|v_{n,out}\right|^2$ – power of input noise voltage.

Transimpedance amplifier sensitivity is defined by the value of input noise current power, photodiode sensitivity, and photodiode dark current (Ahmed, 2013).

Working frequency band Δf defines TIA response time, and the transfer rate of digital signals. As a rule, TIA frequency bandwidth is defined by -3dB level. When bandwidth Δf increases, integral noise current at TIA input rises, and, thus, sensitivity of receiving IC decreases; therefore, when working frequencies rise, it is necessary to use low-noise transistors, and special design and layout solutions. Output power P_{out} (usually, at the 1 dB compression point) defines maximum possible value of voltage range at the load, which is usually 50 Ω for high-speed circuits. Thus, TIA output stage should be matched with 50 Ω. For example, when 1mW of incident optical power is on photodiode with 1 A/B sensitivity, then the 1 mA of photocurrent is generated. With 1 kΩ (or 60 dBΩ) transimpedance gain, 1V mean square value of output voltage shall be obtained (or 13 dBm at 50 Ω load). Usually, TIA have lesser output power of about $P_{out} = 0\ldots5$ dBm, that allows to obtain 0.4 V mean square value of output voltage, or ±0.56 V maximum value of output voltage.

There are often requirements imposed on the form of TIA gain. Hence, TIA shall assure that the slope of photodiode transfer characteristic is compensated, i.e. TIA transfer characteristic should pre-emphasize the upper frequencies of the given range. Fig.3 presents a simplified method for compensating frequency-dependent losses of photodiode.

Fig. 3 – Method for compensating transfer characteristic of photodiode.
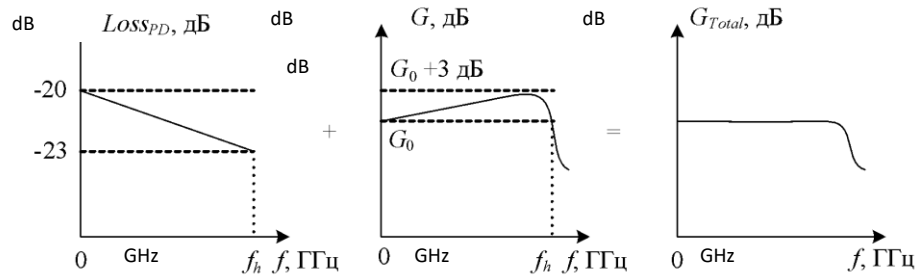
Resistor is the simplest current to voltage converter. Fig.4a presents a diagram of the simplest TIA: a photodiode loaded on resistor. Here, C_{PD} is the photodiode capacitance. Transimpedance gain in this case will be equal to the resistor resistance R_L (Ahmed, 2013; LaFevre, 2011; Cherry & Hooper, 1963). Current is converted into voltage pursuant to Ohm's law.

Fig. 4.

a) Photodiode loaded on resistor. b) equivalent noise circuit of photodiode, loaded on resistor.

a).   b).
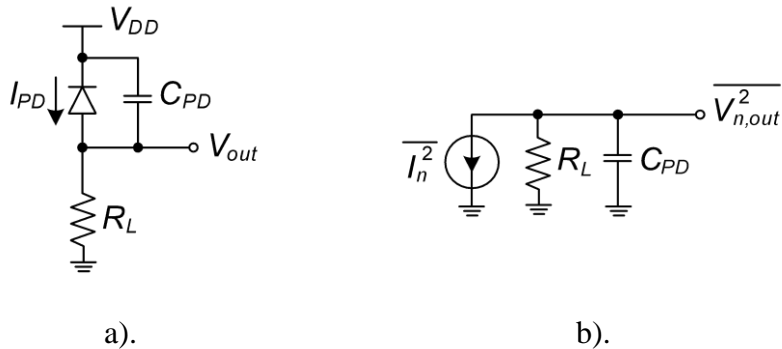
The bandwidth of such circuit will be specified according to the following expression:

$$f_{-3dB} = \frac{1}{2\pi R_L C_{PD}}, \tag{3}$$

where R_L – photodiode load, C_{PD} – photodiode capacitance.

Based on the noise equivalent circuit, depicted in Fig. 5b, power of noise current can be determined:

$$\left| I_{n,in}^2 \right| = \frac{\left| V_{n,out}^2 \right|}{R_L^2} = \frac{kT}{R_L^2 C_{PD}}, \tag{4}$$

where k – Boltzmann constant; T – temperature.

Hence, to increase transimpedance gain, it is required to increase load resistance R_L. At that, according to (3) bandwidth will decrease. An increase in load resistance R_L will entail not only an increase in bandwidth, but also, as per (4), an increase in power of noise current. These simple expressions clearly show compromises between bandwidth, transimpedance gain and noise, faced by engineers when designing TIA. Use of more complex, active circuits allows to widen opportunities provided by this compromise and enhance flexibility of the design.

One of popular circuit of input stage is the use of bipolar transistor (HBT) or field effect transistor (FET), connected with common base/emitter (Fig.5). An advantage of these circuits is low input impedance (~$1/g_m$), due to which there is a matching between photodiode and input stage. It also allows to use photodiode with higher input capacitance. Transimpedance gain will be $Z_T = R_D$ (or R_C, depending on the type of transistor, see Fig.5). However, use of common-gate/base circuit is complicated due to difficulties in achieving simultaneously broad bandwidth and high gain. An increase of resistor R_D/R_C to augment transimpedance gain will cause reduction of voltage on transistor VT1/Q1. Noise characteristics of such circuits also come short of satisfactory (Cherry & Hooper, 1963).

Fig. 5.

a) TIA input stage: a) on FET with common gate.   b) on HBT with common base.


a)   b)
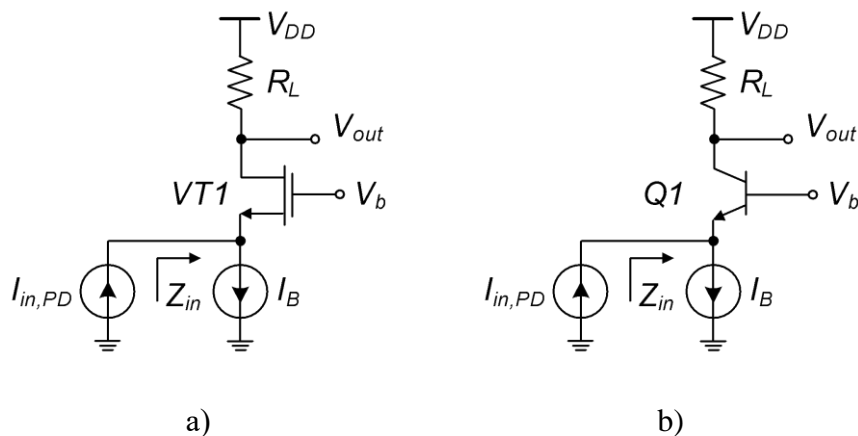
Further improvement of common gate configuration is regulated gate cascode amplifier (RGC), depicted in Fig. 6.

Here, an input resistance is additionally reduced due to adding common source amplifier to the base of transistor VT3. Thus, an input resistance is:

$$R_{in} = \frac{1}{g_{m1}(1+g_{m3}R_g)},\qquad(5)$$

where g_{m1} and g_{m3} – transconductance of transistors VT1 and VT3, respectively, R_g – load resistance for common source amplifier based on transistor VT3.

Fig. 6 –RGC TIA circuit.
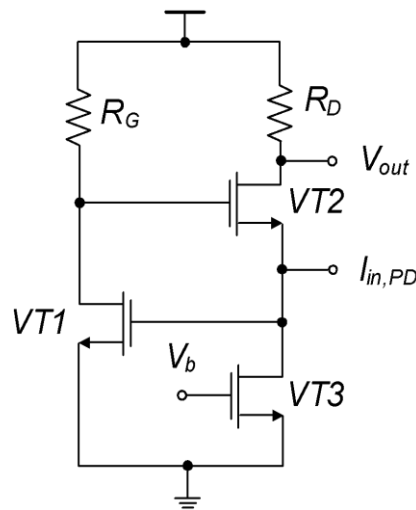
Due to small input resistance this circuit is widely used, when photodiode capacitance is rather large. In general, its shortcomings are similar to those of a common gate circuits.

The use of current negative feedback is the most popular solution in TIAs, see Fig. 7 (Cherry & Hooper, 1963; Kobayashi, 2003).

Low input resistance, feedback resistance R_F with no direct current consumed, and low output resistance constitute advantages of such circuit.

Fig. 7.
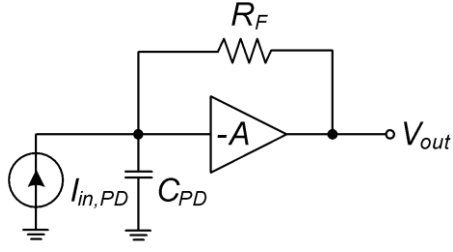
a) TIA with current negative feedback.   **b) equivalent noise circuit.**
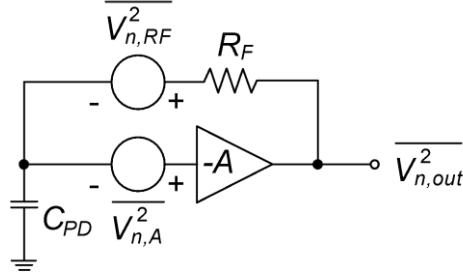
Transimpedance gain of TIA with current negative feedback is:

$$Z_T = -\frac{AR_F}{A+1+j\omega R_F C_{PD}} \sim R_F, \qquad (6)$$

where A – gain; R_F – feedback resistance.

With high values of gain A, transimpedance gain is defined only by feedback resistor R_F.

Bandwidth of this amplifier is determined as follows:

$$f_{-3dB} = \frac{A}{2\pi R_F C_{PD}}. \qquad (7)$$

By assuming that capacitance of photodiode is small ($C_{PD} = 0$), the following expression may be obtained for input noise current:

$$\left| I_{n,in}^2 \right| = \frac{4kT}{R_F} + \frac{\left| V_{n,A}^2 \right|}{R_F^2}, \qquad (8)$$

where $V_{n,A}^2$ – noise voltage at the amplifier input.

As is seen from (8), input noise current may be reduced by increasing feedback resistance R_F, and, thereby increasing transimpedance gain (6). The difference from the common-gate topology is in the fact that an increase in resistance R_F will not result in decreasing voltage drop on amplifying transistor.

Below in Fig. 8, some TIA design solutions are presented based on the amplifier with current negative feedback (see Fig. 7), using the various transistor fabricating technologies.

Fig. 8 –TIA design solutions based on the amplifier with current negative feedback using various transistor fabricating technologies.

a)

b)

c)

d)

e)

f)
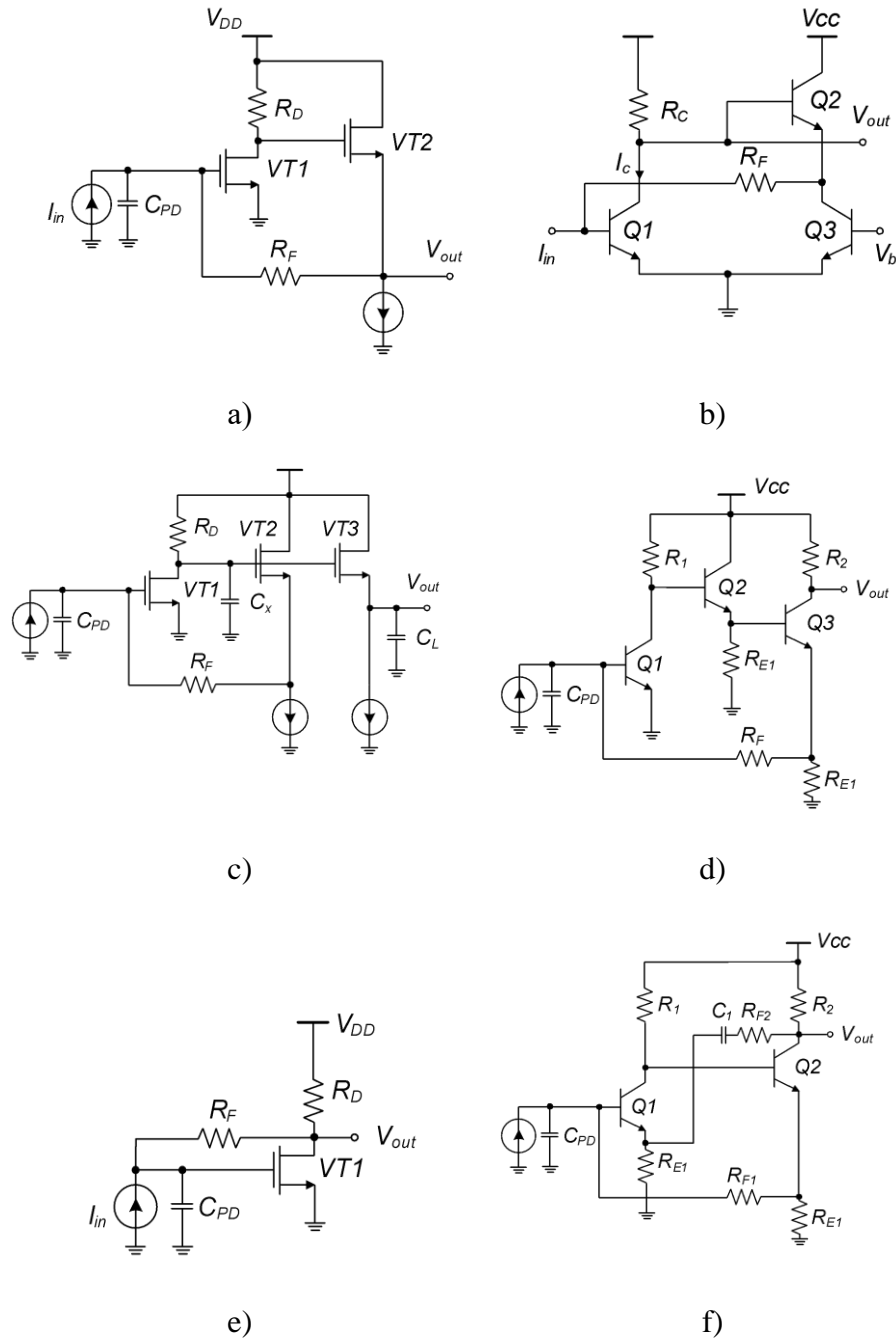
Use of Cherry-Hooper amplifier circuit depicted in Fig. 11, is one of the methods for extending bandwidth and increasing gain of TIA (LaFevre, 2011; Cherry & Hooper, 1963).

Fig. 9.
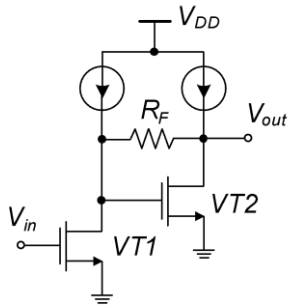
a) Cherry-Hooper amplifier.   **b) simplified equivalent circuit.**
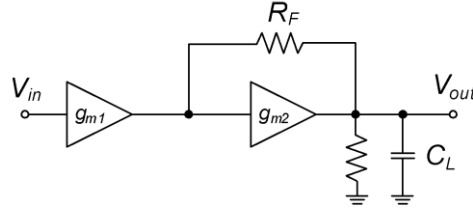
a)   b)

The first stage of Cherry-Hooper amplifier converts input signal into current, the second one with negative current feedback inversely converts signal into voltage. Gain and frequency bandwidth are defined by the following expressions:

$$G = g_{m1}R_F; \quad f_{-3dB} = \frac{g_{m2}}{2\pi C_L}, \qquad (9)$$

where g_{m1} and g_{m2} – transconductance of the first and second amplifier stages, respectively; C_L – load capacitance.

Thus, (9) shows that, as opposed to the previous circuits, frequency bandwidth and gain depend on various values. Particularly, bandwidth depends on the transconductance of the second stage g_{m2} and load capacitance C_L, and gain is defined by feedback resistance R_F and transconductance of the first stage g_{m1} (Kobayashi, 2003).

Results.

Specification of requirements.

The work is intended to design and experimentally investigate an integrated optical receiver (PD+TIA) with 20GHz bandwidth based on 0.25 µm SiGe BiCMOS technology.

Integrated optical receiver should have the following characteristics:

- Bandwidth Δf: not less 20 GHz;

- Wavelength λ: 1550 nm;

- Transimpedance gain Z_T: not less 60 dBΩ;

- Input-referred noise current i_n: not more than 20 pA/$\sqrt{Hz}$:

- Output power P_{out}: not less 0 dBm;

- Output matching $|S_{22}|$: not less -10 dB;

The works related to design and examination of integrated optical receiver involved several stages: 1) development and experimental study of single-stage TIA; 2) development and experimental study of three-stage TIA; 3) development of TIA with integrated PD and compensation circuit of direct current offset.

Development of electrical diagram of single-stage TIA and measurement results.

Fig. 10 presents the circuit schematic of single-stage TIA based on the circuit with parallel current feedback. Resistor R1 specifies TIA transimpedance and input matching. Transistor Q1 is connected in common emitter toplogy, whereas transistor Q3 is connected in common collector topology, i.e. it plays a role of voltage repeater (emitter follower). Transistors Q2, Q3 and resistor R4 specify the operating point of emitter follower. Resistors R2 and R3 define the operating point of transistor Q1, and shunt peaking inductance L1 used to increase the bandwidth of TIA. The value of inductance L1 is very important in terms of amplifier stability. Output signal may be read both from transistor Q2 emitter, and its gate, to ensure DC voltage headroom for the next stage, however, but in that case the gain will be lower. Photo of fabricated single-stage TIA is presented in Fig. 11 (size 0.5$\times$ 0.5 mm^2).

Fig. 10. Circuit schematic of single-stage TIA.
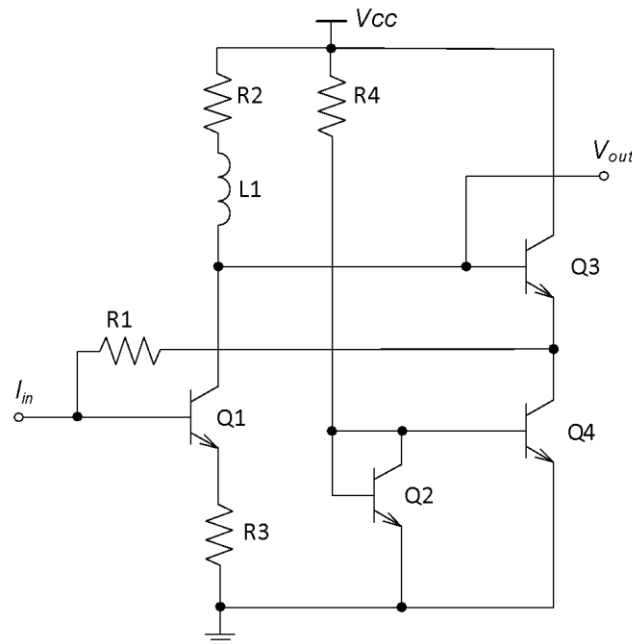
Fig. 11. Die photo of single-stage TIA (size 0.5×0.5 mm^2).
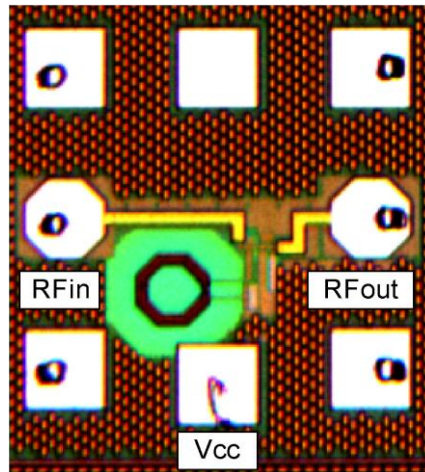
Probe measurements were made using 2-port vector network analyzer ZVA40 and GSG probes with 150 µm pitch. Fig. 12 clearly depicts the results of EM simulation and measurements. Within up to 20GHz bandwidth TIA has a good gain $|S_{21}| = 14 \pm 1$ dB, input coefficient of losses $|S_{11}| < -16$ dB, output reflection coefficient $|S_{22}| < -5$ dB. Since single-stage TIA is an input stage of TIA, it will be loaded for further stage, and output matching is not so important in this case. Transimpedance gain is 48 dBΩ. According to the simulation results, input-referred noise current is 18 pA/√Hz.
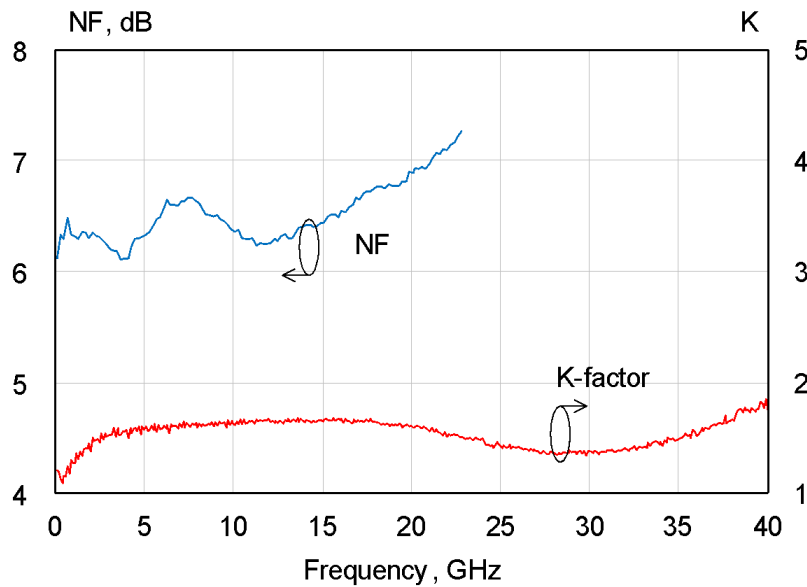
Measured noise figure (NF) is 6-7 dB; group delay is about 14 ± 5 ps. Output power at 1dB compression point at 20 GHz is about to -8.3 dBm. Consumption current is 9 mA, total dissipated power is 23.4 mW.

Fig. 12.

a) Measured and EM simulated S-parameters. b) Measured noise factor and stability K-factor
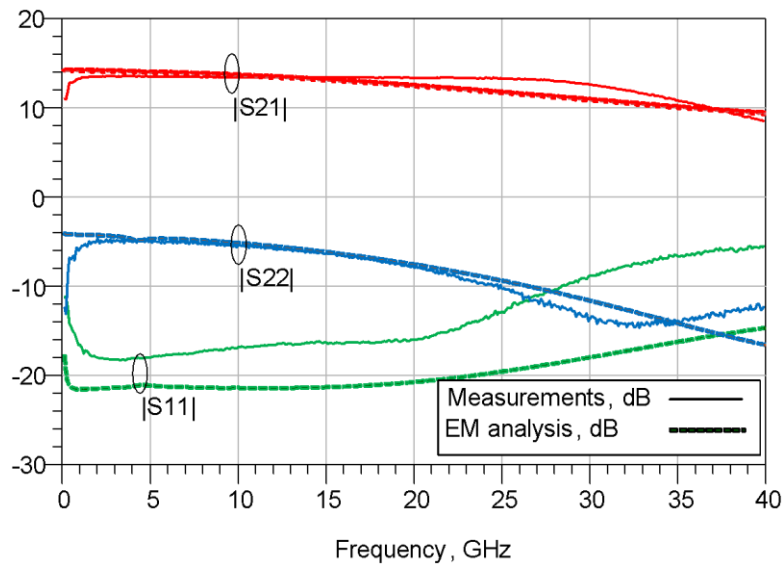
a)

b)

Design of DC-20 GHz three-stage TIA.

The developed integrated TIA consists of three stages: 1) input stage converts PD current to the voltage; 2) post-amplifier gains the signal and transforms it to the differential one; 3) output driver drives the external 50 Ω load and provides the required output power (Fig. 13). A DC offset cancellation loop is also used to compensate DC current from PD.

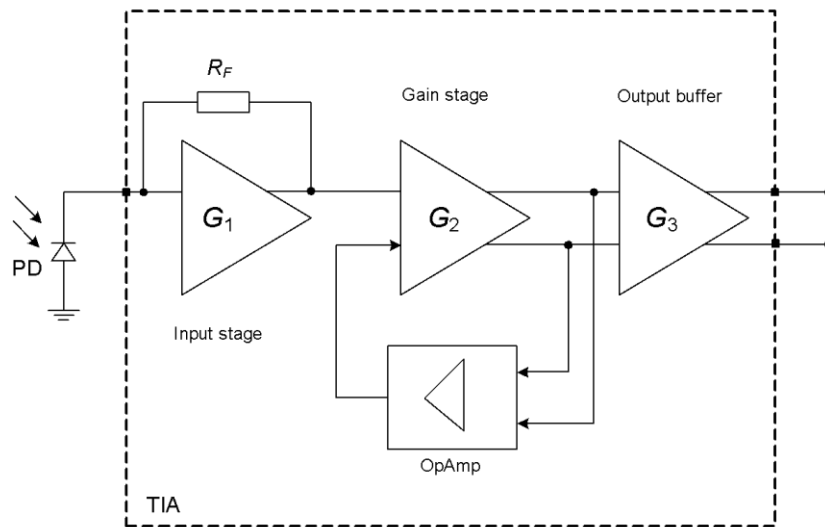**Fig. 13. Structural diagram of TIA with DC-20 GHz bandwidth.**

Fig. 16 presents a circuit schematic of TIA. Input stage (Q1-Q4) is implemented using parallel feedback, resistor R1 specifies TIA transimpedance and input matching. Post-amplifier (Q5-Q16) is made as differential cascode circuit; emitter followers (Q17, Q22) are used for matching with output buffer stage.

Output differential driver (Q23-Q28) contains RC degeneration circuit to compensate TIA gain roll-off and control the PD conversion gain. Operational amplifier (OpAmp) is made on CMOS transistors. Operational amplifier is designed with using CMOS transistors. Low frequency RC circuits are used to eliminate the influence of DC cancellation loop on TIA performances.
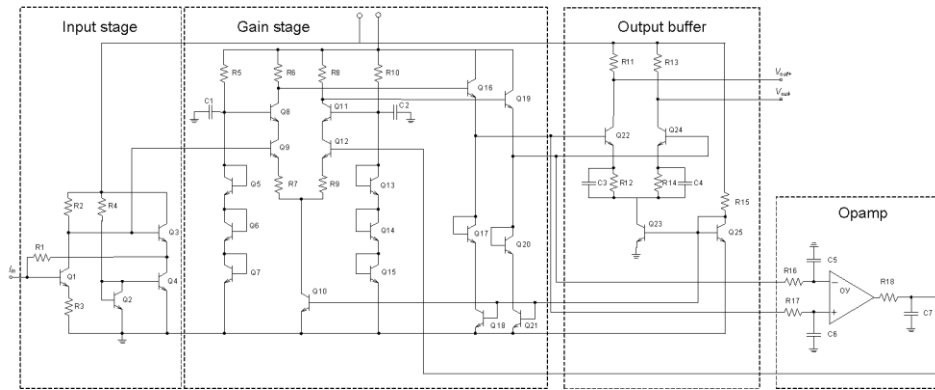
**Fig. 14. Circuit schematic of TIA with DC-20 GHz bandwidth.**

Fig. 15 present characteristics of TIA after EM analysis: S-parameters (Fig. 15a), and calculated transimpedance gain (Fig. 15b).

The results of simulation are: gain $|S_{21}|$ within DC-20 GHz bandwidth varies from 21 dB to 24 dB, while transimpedance gain is about 63 dBΩ. Output power of one TIA channel is -8 dBm. Output matching $|S_{22}|$ varies from -25dB to -10.5 dB, input matching $|S_{11}|$ – from -15 dB to -9 dB. Consumption current is 60 mA (supply voltages are 2.5 V and 3.3 V).
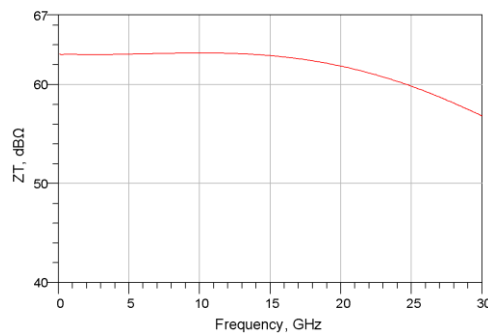
Fig. 15.

a) EM simulated S-parameters of TIA.   **b) calculated transimpedance gain Z_T**
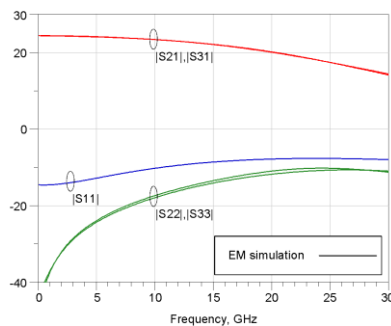
a)   b)

Experimental study of three-stage DC-20 GHz TIA.

The designed three-stage TIA was fabricated based on 0.25 µm SiGe BiCMOS technology (IHP, Germany). Chip measurements were performed at Cascade probe station using 4-port vector network

analyzer ZVA40 up to 40GHz using differential GSGSG-probes with 150µm pitch. Fig.16 presents

a die photo of TIA. Sizes of three-stage TIA are 0.7×0.6 mm^2.

Fig. 16. Photo of integrated circuit of three-stage DC-20 GHz TIA (sizes 0.7×0.6 mm^2)
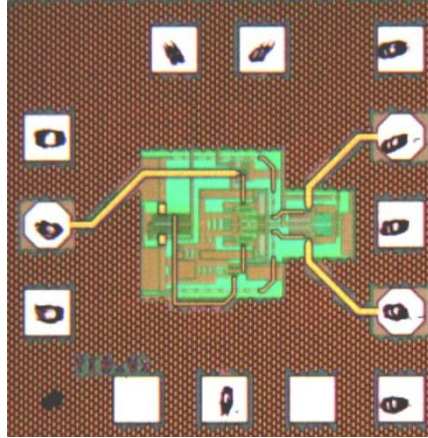

Fig. 17 presents the measured TIA S-parameters. Fig.5 also presents transimpedance gain, calculated

using measured S-parameters. As can be seen, bandwidth at -3 dB cut-off level is about 15 GHz, gain

$|S_{21}|$ is 25±1 dB up to 10 GHz bandwidth, output reflection coefficients $|S_{22}|$ and $|S_{33}|$ is less than -10

dB up to 5 GHz and less than -6 dB on average within up to 15 GHz bandwidth, however, matching

can be improved by using output series inductance. Transimpedance gain Z_T is about 58-65 dBΩ.

The results of measurement differ from simulated due to incorrect layout of active and passive

elements on integrated circuit, and inaccuracy of the EM analysis, what was taken into consideration

during further development activities.

Fig. 17. Measured S-parameters (a) and TIA transimpedance gain (b)

a   b
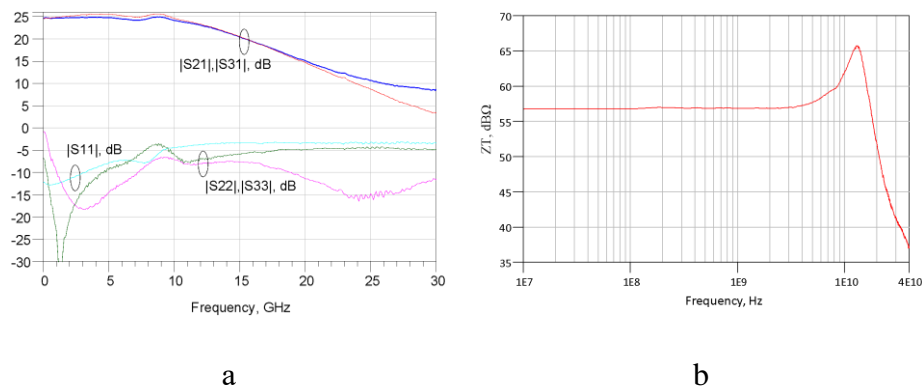
Design of integrated optical receiver with DC-20 GHz bandwidth.

Optical signal induces a current in photodiode, which is further transformed into voltage using TIA. Losses of optoelectronic conversion in photodiode are about 21-25 dB, respectively, TIA should compensate these losses and gain the useful signal.

When frequency of input signal rises, losses of photodiode conversion increase, hence, the developed TIA should compensate these frequency dependent losses through introducing some correction circuits. Usually, this is a frequency dependent negative feedback, use of inductance in the amplifier stage load circuit, impedance matching, etc. Use of integrated inductances considerably increases IC area, hence, in this work a solution was made to refuse from using them.

To design an optical receiver, the results were used, obtained during designing three-stage TIA. The optoelectronic S-parameters of photodiode were provided for by IHP factory. After photodiode and TIA were connected, characteristics of optical receiver were optimized to comply with the specified requirements: gain up to 20 GHz, input-referred noise current i_n, output matching, output power.

In Fig. 18, gain of optical receiver up to 20 GHz is about 2-3 dB, output reflection coefficient $|S_{22}|$ is less than -10 dB.

Output power at 20 GHz for each differential output is -7.5 dBm, that will amount to about -4.5 dBm from fully differential output, mean square amplitude on 50 Ω load is 0.3 V. Transimpedance gain is 61-64 dBΩ or 1500 Ω, and group delay is 30±2 ps (Fig. 19).

Fig. 18. Simulated S-parameters of optical receiver (TIA with integrated PD).
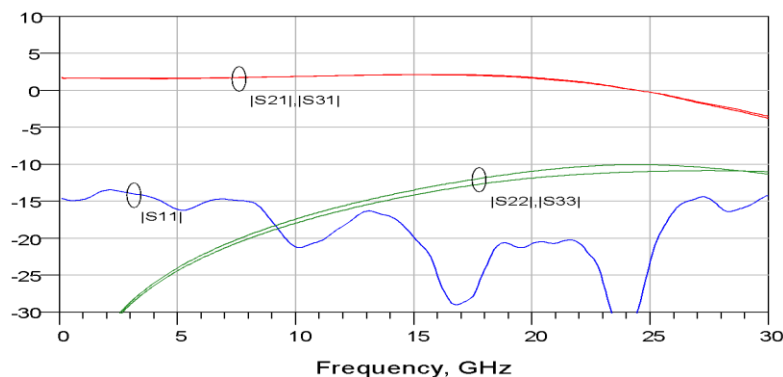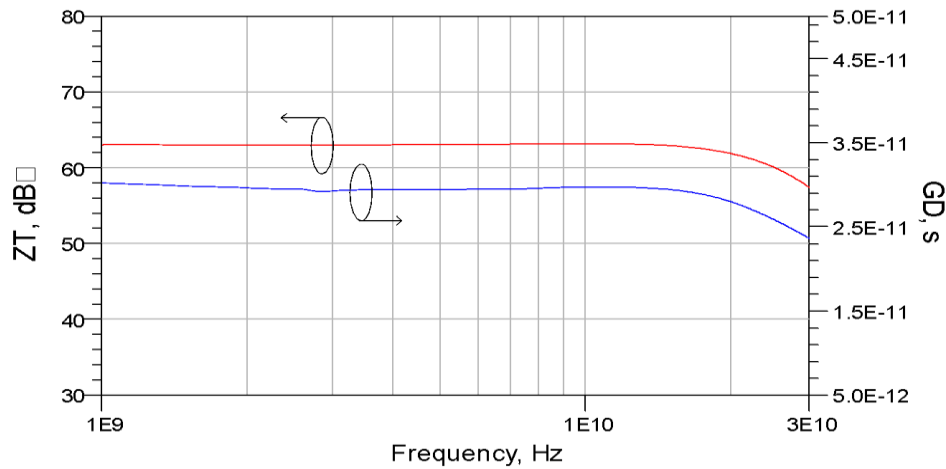
Fig. 19. Transimpedance gain and group delay of DC-20GHz optical receiver.

The topology of a single-chip integrated optical receiver, based on 0.25 µm SiGe BiCMOS technology, is depicted in Fig. 20. A grating coupler designed to minimize losses at 1550 nm is used to inject input optical signal. The bias supply circuit for photodiode was integrated on IC. The sizes of integrated optical receiver are 1.46×0.85 mm^2.

Fig. 20. Layout of single-chip integrated optical receiver (sizes 1.46×0.85 mm^2).
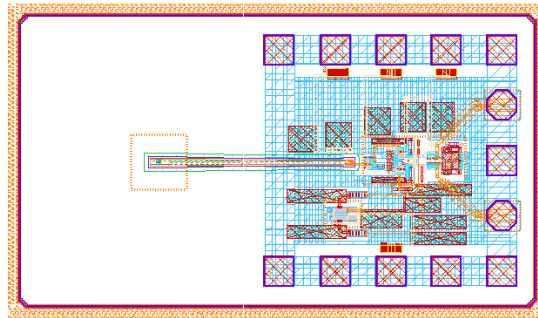
DISCUSSION.

Table 1 presents various optical integrated receivers and TIA integrated circuits with more than 10 GHz bandwidth. The designed optical receiver has, according simulation the lowest value of input-referred noise current i_n. Despite using the technology with 0.25 µm layout rule, the bandwidth of the presented chip is at the level of analogues that are based on the more advanced technologies: 130 nm

CMOS, 130 nm BiCMOS, 90 nm CMOS, 65 nm CMOS (Soref, 2006; Liao & Liu, 2008; Takemoto et al, 2009; Susilawti et al, 2017).

Table 1. Table of integrated optical receivers and TIAs with more than 10 GHz bandwidth.

Ref.	BW, GHz	Z_T, dBΩ	P_D, mW	i_n, pA/√Hz	Technology	Sizes (with pads), notes
[20]	20	75	48	40	130 nm CMOS	$0.8*1.2$ mm^2, optical transceiver
[21]	47	49	73	16.3	0.25 um SiGe BiCMOS	$1.1*1.1$ mm^2, Inductor peaking technique
[22]	15	61	32	22	0.18 um SiGe BiCMOS	$0.54*0.55$ mm^2, Inductor peaking technique
[23]	22	66	75	22	90 nm CMOS	$0.86*0.65$ mm^2, Inductor peaking technique
[24]	31	70	275	28.1	0.25 um SiGe BiCMOS	$3.2*1$ mm^2, Inductorless
[25]	37.6	75.5	150	20	0.25 um SiGe BiCMOS	$1*0.5$ mm^2, Inductor peaking technique
[26]	20	70	74	22.6	65 nm CMOS	$0.5*0.715$ mm^2, Inductor peaking technique
This work	25	63	200	15.6	0.25 um SiGe BiCMOS	$1.46*0.85$ (with optical pads) Inductorless

CONCLUSIONS.

The developed integrated optical receiver, comprising photodiode and transimpedance amplifier, has DC-20 GHz bandwidth. According to the results of simulation, gain up to 20 GHz is about 22-25 dB, transimpedance gain is 61-65 dBΩ, consumption current is 60 mA. Output power at 20 GHz is -4.5 dBm, mean-square range of amplitude is 0.3 V on 50 Ω load, input-referred current noise i_n = 15.6 pA/√Hz. The designed integrated optical receiver could be used in many applications: transmitting

of microwave signals inside large objects, electronic warfare systems (EWS), optical lines of delaying and processing signals, AESA, broadband communications.

BIBLIOGRAPHIC REFERENCES.

1. Seeds, A. J. (2002). Microwave photonics. IEEE Transactions on Microwave Theory and Techniques, 50(3), 877-887.

2. Capmany, J., & Novak, D. (2007). Microwave photonics combines two worlds. Nature photonics, 1(6), 319.

3. Coldren, L. A. (2010, October). Photonic integrated circuits for microwave photonics. In Microwave Photonics (MWP), 2010 IEEE Topical Meeting on (pp. 1-4). IEEE.

4. Awny, A., Nagulapalli, R., Winzer, G., Kroh, M., Micusik, D., Lischke, S., & Zimmermann, L. (2015). A 40 Gb/s Monolithically Integrated Linear Photonic Receiver in a $0.25~\mu {\rm m}$ BiCMOS SiGe: C Technology. IEEE Microwave and Wireless Components Letters, 25(7), 469-471.

5. Rito, P., López, I. G., Petousi, D., Zimmermann, L., Kroh, M., Lischke, S., ... & Kissinger, D. (2016). A Monolithically Integrated Segmented Linear Driver and Modulator in EPIC 0.25-μ m SiGe: C BiCMOS Platform. IEEE Transactions on Microwave Theory and Techniques, 64(12), 4561-4572.

6. López, I. G., Rito, P., Micusik, D., Borngräber, J., Zimmermann, L., Ulusoy, A. C., & Kissinger, D. (2015, May). A 2.5 Vppd broadband 32 GHz BiCMOS linear driver with tunable delay line for InP segmented Mach-Zehnder modulators. In Microwave Symposium (IMS), 2015 IEEE MTT-S International (pp. 1-4). IEEE.

7. Assefa, S. (2013). Integration of silicon photonics in bulk CMOS, IEEE International Electron Devices Meeting (EIDM).

8. Razavi, B. (2012). Design of integrated circuits for optical communications. John Wiley & Sons.

9. Yao, J. (2009). Microwave photonics. Journal of Lightwave Technology, 27(3), 314-335.

10. Jalali, B. (2006). Silicon photonics. IEEE Microwave Magazine, 7(3), 58–68

11. Soref, R. (2006). The past, present, and future of silicon photonics. IEEE Journal of selected topics in quantum electronics, 12(6), 1678-1687.

12. Jalali, B., & Fathpour, S. (2006). Silicon photonics. Journal of lightwave technology, 24(12), 4600-4615.

13. Dumon, P., Bogaerts, W., Baets, R., Fedeli, J. M., & Fulbert, L. (2009). Towards foundry approach for silicon photonics: silicon photonics platform ePIXfab. Electronics letters, 45(12), 581-582.

14. Leijtens, X. (2011). JePPIX: the platform for Indium Phosphide-based photonics. IET optoelectronics, 5(5), 202-206.

15. Wang, Z. (2018). Brief Introduction of High-Speed Circuits for Optical Communication Systems [online resource], Accessibility mode: www.ee.buffalo.edu/faculty/paololiu/566/wang.ppt free (date of reference: 20.01.2018)

16. Ahmed, M. N. (2013). Transimpedance amplifier (TIA) design for 400 Gb/s optical fiber communications (Doctoral dissertation, Virginia Tech).

17. LaFevre, K. (2011). Design of a Modified Cherry-Hooper Transimpedance Amplifier with DC Offset Cancellation. Arizona State University.

18. Cherry, E. M., & Hooper, D. E. (1963, February). The design of wide-band transistor feedback amplifiers. In Proceedings of the Institution of Electrical Engineers (Vol. 110, No. 2, pp. 375-389). IET Digital Library.

19. Kobayashi, K. W. (2003, June). State-of-the-art 60 GHz, 3.6 k-Ohm transimpedance amplifier for 40 Gb/s and beyond. In Radio Frequency Integrated Circuits (RFIC) Symposium, 2003 IEEE (pp. 55-58). IEEE.

20. Liao, C. F., & Liu, S. I. (2008). 40 Gb/s transimpedance-AGC amplifier and CDR circuit for broadband data receivers in 90 nm CMOS. IEEE Journal of Solid-State Circuits, 43(3), 642-655.

21. Takemoto, T., Yuuki, F., Yamashita, H., Ban, T., Kono, M., Lee, Y., ... & Nishimura, S. (2009, September). A 25-Gb/s, 2.8-mW/Gb/s low power CMOS optical receiver for 100-Gb/s Ethernet solution. In Optical Communication, 2009. ECOC'09. 35th European Conference on (pp. 1-2).

22. Susilawti, W., Suryadi, D., & Dahlan, J. A. (2017). The Improvement of Mathematical Spatial Visualization Ability of Student through Cognitive Conflict. International Electronic Journal of Mathematics Education, 12(2), 155-166.

DATA OF THE AUTHORS.

1. Artyom S. Koryakovtsev. Tomsk State University of Control Systems and Radioelectronics (TUSUR),40, Lenin Avenue, Tomsk, 634050, Russia. Email: tintartyom@mail.ru

2. Andrey A. Kokolov. Tomsk State University of Control Systems and Radioelectronics (TUSUR),40, Lenin Avenue, Tomsk, 634050, Russia. Email: kokolovaa@gmail.com

3. Alexey V. Pomazanov. Tomsk State University of Control Systems and Radioelectronics (TUSUR),40, Lenin Avenue, Tomsk, 634050, Russia.

4. Feodor I. Sheyerman. Tomsk State University of Control Systems and Radioelectronics (TUSUR),40, Lenin Avenue, Tomsk, 634050, Russia.

5. Leonid I. Babak. Tomsk State University of Control Systems and Radioelectronics (TUSUR),40, Lenin Avenue, Tomsk, 634050, Russia.